JOURNAL OF MARINE SCIENCES & ENVIRONMENTAL TECHNOLOGIES
Vol. 7, Issue No. 2 (December-2021)

ISSN (Print): 2413-5267
ISSN (Online): 2706-9966

Determine of Nitrogen Dioxide Emissions over Khuoms City in Libya Using MODIS and TROPOMI Satellites

Dawi Muftah Ageel

Department of Geology and Environmental Science, Faculty of Sciences, Elmergib University, Khuoms, Libya.

E-mail: dmageel@elmergib.edu.ly

كشف انبعاثات ثاني أكسيد النيتروجين فوق مدينة الخمس في ليبيا باستخدام القمرين الصناعيين موديس وتروبومي

الضاوي مفتاح عقيل

قسم علوم الأرض والبيئة، كلية العلوم، جامعة المرقب، الخمس، ليبيا.

Received: 17 October 2021; Revised: 19 November 2021; Accepted: 01 December 2021.

Abstract

Sentinel-5 Forerunner (S-5P), carrying the TROPO round recognition Instrument (TROPOMI) nadir-viewing crystal spectroscope, is that the beginning mission of the Copernicus Program committed to the recognition of air quality. Within the given data the TROPOMI tropospheric gas (NO_2) level-2 (L_2) item has been substantially over capably sullied urban districts by comparison with coincident high-resolution MODIS remote detecting observations (1 km×1 km). Satellite products may be ideally surveyed backed by 5 bands, as an out-measured amount of lackey pixels may be completely mapped within the system of the S-5P approval campaign over Khumos town in Libya. Each piece of information was taken in 2020 over a power station in Khuoms city in Libya, for mapping the level dissemination of tropospheric NO_2, each image pixel was fully covered by approximately 370 to 700 nm for visible spectrum (MODIS and TROPOMI pixels). The TROPOMI and MODIS NO_2 emissions were similar in concept, the regression analysis of both data with well correlated (R^2= 0.87), and there is a negative relationship (-0.03×10^{15} molec/cm^2) recorded when clouds and dust were prevalent over the study area. From the results obtained from MODIS and TROPOMI data, nitrogen dioxide emissions were high to medium (6.6 to 3.2×10^{15} molec/cm^2) at their source and five kilometers from the source, while the rest of the study area ranged from (2.2 to 0.15×10^{15} molec/cm^2) low to very low.

***Keywords**: TROPOMI, MODIS, Khuoms, Libya.*

الملخص

القمر الصناعي سينتينال (5-إس) هو أداة متطورة لمعاينة جودة الهواء بواسطة الطيف البلوري لذلك التلوث والذي يعرف بـ(TROPOM)حيث يحمل المطياف البلوري (TROPOMI)، وهو المهمة الأولى لبرنامج كوبرنيكوس المتخصص في الكشف عن جودة الهواء. كانت البيانات المعطاة تشير إلى معدلات عالية إلى متوسطة من غاز ثاني أكسيد النيتروجين في المناطق الحضرية مقارنةً بالمعدلات المرصودة أبعد من تلك المناطق. الرصد كان باستخدام قياسات عالية الدقة من القمر موديس (MODIS) الذي يمتلك قوة بيكسل تصل إلي (1كم×1 كم) و5 نطاقات طيفية تتطابق وتدعم قياسات المطياف تروبومي (TROPOMI)، تمت تجربة بيانات كلا القمرين على مدينة الخمس في ليبيا، وتم أخذ البيانات في عام 2020 من محطة الطاقة الغازية الواقعة قريباً من مركز مدينة الخمس، لرسم خرائط مستوى انتشار ثاني أكسيد النيتروجين في التروبوسفير لموقع المدينة، تمت تغطية كل

ISSN (Print): 2413-5267
ISSN (Online): 2706-9966

بكسل صورة بالكامل بحوالي 370 إلى 700 نانومتر للطيف المرئي حيث كان تحليل الانحدار الخطي لكل منهما إيجابيًا (R^2=0.87)، وكانت هناك علاقة سلبية (-0.03×10^{15} جزيء/سم^2) سجلت عندما كان طقس سائداً بالغبار أو السحب خلال منطقة الدراسة. من النتائج التي تم الحصول عليها من بيانات القمرين كانت انبعاثات ثاني أكسيد النيتروجين عالية إلى متوسطة (7.2 إلى 4.3×10^{15} جزيء/سم^2) عند مصدرها وبقطر خمسة كيلومترات من المصدر، بينما تراوحت ببقية منطقة الدراسة (من 3.2 إلى 0.15×10^{15} جزيء/سم^2) منخفض إلى منخفض جدًا.

الكلمات الدالة: تروبومي، موديس، الخمس، ليبيا.

1. Introduction

1.1. Effects of NO_2

1.1.1. Health effects

High concentrations of NO_2 effecting on breathing air of the human respiratory system with ability on irritate airways. Thus, it leads to serious respiratory problems such as asthma when exposed to this pollutant for short periods. Also, coughing, wheezing, or difficulty breathing diseases. The elderly and children due to immunodeficiency are more exposed to this pollutant (NO_2) than other groups. In addition, nitrogen dioxide deposits affect the metabolic processes of hemoglobin and the exchange of oxygen at high concentrations of this pollutant, which leads to nitrogen poisoning. It also effects on the functioning of neurons, which contributes to mental illnesses such as insomnia, depression and anxiety (Ibrahim *et al*., 2011; Ibrahim *et al*. 2012a; Ibrahim *et al.*, 2012b, and EPA, 2016).

1.1.2. Environmental effects

The physical properties of nitrate oxides are colorless and react with water vapor in the atmosphere or air to form nitrogen dioxide. Nitrogen dioxide has a distinctive odor and is impure, acidic and highly corrosive, affecting the surrounding environment. It produces yellowish-brown smog, which is toxic to the marine, plant and population environment. Household appliances such as heaters and heaters are a major source of nitrogen oxides, which makes the internal environment of the house polluted, toxic, and causes many diseases for the residents of those poorly ventilated dwellings. (EPA, 2018).

1.2. Data

1.2.1. MODIS imagery

NASA launched the Moderate Resolution Imaging Spectroradiometer (MODIS) sensor in 1999 by Terra (EOS AM) and then by Aqua (EOS PM) in 2002. Its data captures about 36 spectral bands, wavelengths between 0.4 and 14.4 µm and in degrees Varying spatial (2 bands at 250 metres, 5 bands at 500 metres, and 29 bands at 1 kilometer) (Morisette *et al*., 2012).

The MODIS satellite monitors the Earth daily, recording weather fluctuations and exposure of the atmosphere to solar and cosmic radiation, as well as ecological processes of ocean biomass and earth. MODIS uses four calibrators that include: a solar diffuser (SD), a solar diffuser stability monitor (SDSM), a Radiation Spectrum Calibration Kit (SRCA), and a black-body v-groove calibrator (Justice *et al*., 2015). A marine optical buoy was one use of the MODIS indirect calibration. MODIS has added VIIRS calibrators for the 2011 Suomi

ISSN (Print): 2413-5267
ISSN (Online): 2706-9966

NPP and Joint Polar Satellites (JPSS). It is of high quality and supports advanced geophysical processes (Friedel *et al*., 2017). MODIS satellite data covers the entire Earth every two days, covering the measurement of climatic fluctuations in the atmosphere, its exposure to solar and cosmic radiation, as well as the environmental processes of biomasses in the oceans and land. MODIS uses four calibration devices that include: a solar diffuser (SD), a solar disperser stability monitor (SDSM), a Radiation Spectral Calibration Kit (SRCA), and a black-body v-groove calibrator (Justice *et al.*, 2015). The marine optical buoy was one of MODIS's indirect calibration uses. MODIS added the VIIRS calibrators for the 2011 Suomi NPP and Joint Polar Satellites (JPSS). It is of high quality and supports advanced geophysical processes (Friedl *et al.*, 2017).

1.2.2. TROPOMI

TROPOMI data is based on DOMINO V2 and QA4ECV climate variability processing technologies, with a number of technologies important to the work of TROPOMI (Boersma *et al.*, 2018), using a 3D parallel system on MP data to process data obtained from periodic data. Journal, Version 5 (TM5) of the Transfer Model (CTM) (Huijnen *et al.*, 2016) it follows a three-step approach:

- Detection of NO_2 emissions along the light path used by DOAS method (Platt & Stutz, 2014) at the level of the spectral radiation of the single link and the multispectral radiation of TROPOMI. DOAS exploration is based on nonlinear recording of data (Van Noije *et al.*, 2006), and uses SCDs to monitor the optical path through the atmosphere based on the geometry of vision, the prevailing atmospheric condition, and the solar radiation transmitted through it. Radiation reflected through the atmosphere and penetrating the troposphere is precisely recorded by SCDs (Williams *et al.*, 2017).
- After the information is recorded by SCD technology, the data is stored on VCDs, which include the air masses associated with the recording period (AMFs). The AMFs illustrate the relationship between solar beam geometry and the vertical distribution of NO emissions, surface albedo, cloud height, aerosol scattering, and the nature of the terrain. All of these data are obtained by the integrated product of (1) daily vertical-measured AMFs of the TM5-MP model on a 1×1 grid covering 34 vertical layers (between surface and upper atmosphere; TOA). Square AMFs are calculated based on the KNMI-add multiplexing (DAK version 3.2) radiative transfer mode (RTM) (Griffin *et al.*, 2019; and Ortega *et al.*, 2015). The TROPOMI climatology data from 5 years ago is based on data aggregated in a 0.5×0.5 grid (Van Geffen *et al.*, 2020). For nitrogen dioxide detection techniques, the Lambert reversal (LER) model is used. LER is defined as the surface corresponding to the required reflection according to that available TOA model under scattering conditions, i.e. clouds and aerosols. Indications for withdrawal are explored from the algorithm for calculating the availability of oxygen in the target range (Vasilkov *et al.*, 2017).

Algorithms used to detect NO_2 emissions in TROPOMI technologies are defined using TM5-MP CTM technology, an improvement over the TM4 CTM, and run for OMI DOMINO

ISSN (Print): 2413-5267
ISSN (Online): 2706-9966

v2.0. It contains a large spatial resolution (1×1), clearer information on nitrogen oxide emissions, photolysis and detection of chemical interaction of emissions with atmospheric components (Van Geffen *et al.*, 2020), where a gradient is observed in highly contaminated areas Nitrogen vertically and horizontally (Pinardi *et al.*, 2020). These pollutant gradients cannot be measured over an area of 100×100 kilometer square (Dimitro *et al.*, 2020).

Sentinel-5 Precursor (S-5P) is one of the products of the European Aerospace by Copernicus Company to monitor the atmosphere, and what it contains from natural phenomena such as weather, hurricanes and industrial such as climate change, the pollutant concentrations and their types. It was launched in October 2017 and it is still working well and accurately, and depends on it in the environmental studies. It carries the TROPO Isotope Display Spectrometer (TROPOMI) as its single payload. TROPOMI provides measurements of atmospheric composition with an unprecedented combination of resolution, spatial coverage and spatial resolution, providing new opportunities such as studying the diversity of pollutants on a city scale, as well as monitoring the global distribution of gases (Compernolle *et al.*, 2020).

The new sensor technology and the method of exploration need to evaluate the effectiveness and importance of the data produced in terms of accuracy and that it meets the requirements of the required scientific research, in comparison with the existing data and available technical capabilities. TROPOMI's operational superiority lies in high quality, long-term routine monitoring of Level 1 (L_1) and Level 2 (L_2) (Ialongo *et al.*, 2019). Troposphere NO_2 is one of the main monitored gas products by TROPOMI. It is a major pollutant of the environment and has a direct impact on human health, attaching to the ozone layer and particulate matter. NO_2 is formed from nitrogen monoxide (NO) and then rapidly oxidized to NO_2 by its reaction with oxygen in urban air, the primary source being combustion fuels due to traffic, home heating and industrial activities. Nitrogen dioxide is a short-lived species with a lifespan of approximately hours. Its distribution is characterized by a strong spatiotemporal variability when approaching emission sources (Kim *et al*., 2016).

TROPOMI is most suitable for monitoring emissions and sources of nitrogen dioxide in urban areas and at short wavelengths (Kleipool *et al.*, 2018). Previous studies focus on evaluating the TROPOMI L_2 tropospheric NO_2 product in continental polluted areas in general, but with this product it allowed accuracy in the results for less area polluted areas due to TROPOMI's limited lunar pixel size, which is usually much lower than heterogeneous pollution plume gradients. For example, a single isotope TROPOMI pixel of 3.5 km by 7 km has about 280 pixels (Constantin *et al.*, 2016).

For the detection of NO_2 emissions by TROPOMI techniques in polluted areas and compare these data with MODIS sensor. By satellite pixel of each satellite image which were sampled from the target regions. This comparison as made by several previous studies such as Lamsal *et al*. (2017) and Heue *et al*. (2018). The validity and high quality of these comparisons were confirmed. Due to the large pixel footprint of the TROPOMI sensor in areas also covered by MODIS fingerprints. The TROPOMI instrument is a visible ophotometer by the Netherlands Space Office (NSO), the Royal Netherlands specter Meteorological institute (KNMI), the

ISSN (Print): 2413-5267
ISSN (Online): 2706-9966

Netherlands institute for Space Research Organization (TNO) and ESA ogiestechnolworkare similar to the SCIAMACHY sensor o Envisat's by ESA agency and OMI on NASA's Aura satellite (Levelt *et al*., 2006).

The main objective of the lunch of the TROPOMI sensor is for tasks of making atmospheric measurements related o air quality, climate impact, zone, and ultraviolet radiation decessors in ESA and TROPOMI bridges the gap in continuity of observations between its permissions (Broccardo *et al*., 2018; and 4-Sentinel & 5-upcoming Sentinel). The TROPOMI sensor consists of four spectrophotometers covering the UV-VIS-NIR-SWIR wavelength ranges with a spectral resolution ranging from 0.45 to 0.65 nm in the UV-VIS range. TROPOMI is located in a semi-polar sun-synchronous orbit at an altitude of 824 km with a tropical ascending node at 13:30 GMT. The portal telescope allows a wide field of view (FOV) of 108°, corresponding to a flat width of about 2,600 km, providing daily global coverage with a ground pixel size of about 3.5 km×7 km at perihelion (Zhao *et al.*, 2020).

2. Method and Materials

2.1. Study area

The power plant in Khuoms is the main source of nitrogen oxides (NOx= NO+NO_2). When the wind blows, plumes can be observed near the shores of Khuoms, and on this basis, the Khuoms Power Plant (KPP) has been identified as a major problem in producing nitrogen dioxide (NO_2) pollutants. TROPOMI techniques were used in this study because of the observed urban damage from the nitrogen dioxide emissions of this station. The importance of the superior technologies of the TROPOMI sensor in the field of studying these pollutants, and aavailability of MODIS hyper spectral images complementary to TROPOMI data at similar wavelength functions. Study area about (1,753 km^2) as shown in Figure (1), this area covers the emission source.

The TROPOMI data pixels were used for statistical data to each single image. MODIS data were tabulated and the temporal variance reduction with the TROPOMI data for investigates from NO_2 emissions to both satellites. The data occurred in mostly cloud-free conditions and on days with good visibility (12% withdrawal percentage). During all study days there was recorded light emission between 0.3 and 0.7 mol/m^2 KPP, based on the average wind speed during the time of flight, the winds were usually blowing from the north and northwest, and there was a strong northwest wind. Wind data was collected from the Advanced High Resolution Radiometer (AVHRR) which is used to generate latitude wind field features in the visible spectrum window bands. All observations were made in the solar noon period. The favorable position of the sun during summer maximizes the light reflected off the sensor and reduces the signal smoothing that occurs at shallow sun elevation angles. On the other hand, the total NO_2 signal is generally lower during the summer due to the shorter lifetime of NO_2 (Lawrence *et al.*, 2015).

ISSN (Print): 2413-5267
ISSN (Online): 2706-9966

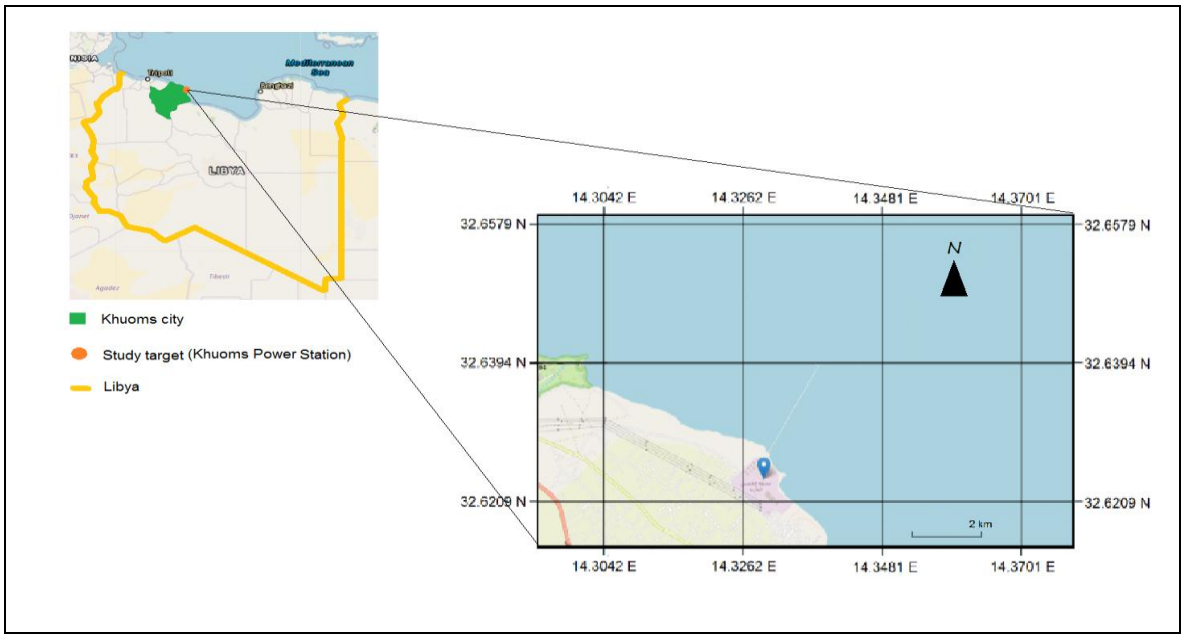

Figure 1. Study location from the northern part of Khuoms city.

2.2. Statistics

2.2.1. Regression method

Regression analysis is a statistical tool that investigates relationships between variables. Usually, the researchers seek to ascertain the causal effect of independent variables **Y** upon dependent variables $\mathbf{x_i}$ (Van Noije *et al*., 2006). When we use the model to forecast y for a particular set of values of $\mathbf{x_i}$, it need to measure how large the error of the forecast might be. All these elements, including dependent and independent variables and error, are part of a regression analysis, and the resulting forecast equation is often called a regression model (Van Geffen *et al.*, 2021). Regression analysis is a basic technique in air pollution forecasting. Linear regression plays a strictly utilitarian role in the field of statistical methods. Its expression as given by Eqn. (1):

$$Y=b_0+b_1x+e \quad \ldots\ldots \quad (1)$$

The TROPOMI emission data have compared with Moderate Resolution Imaging Spectroradiometer (MODIS) emission data and more specifically with regression line analysis. When comparing TROPOMI and MODIS emission the range value is much lower (-zero) for better comparison between both data emissions, and the similar values were found when comparing the data with same time. The emission is wavelength dependent and emission products at different wavelengths have been compared: MODIS at 550 nm, and TROPOMI emission at 480 nm. The observed overestimation of the NO_2 seems to be consistent with comparison studies reported by Kleipool *et al*. (2018). According to Kleipool *et al*. (2018), this is partly related to viewing reflectance effects of the surface. The

ISSN (Print): 2413-5267
ISSN (Online): 2706-9966

TROPOMI and MODIS products are also not provided at the same wavelength, and time series analysis is used to determine the reflectance value.

2.2.2. Support vector regression

Support vector regression (SVR) is the implementation of support vectors in a regression function. SVR has the advantages of measuring the space of the measured and comparative dimensions and it depends on the optimization of the dimensions of the space of the input values (Hong *et al*., 2015). In the high-dimensional feature space, there is a linear function, which maps the input data to a two-dimensional space through a line graph. This linear function is known as the SVR equation [Eqn. (2)] (Shi *et al.*, 2008):

$$f(x) = (wx) + b \quad \ldots\ldots \quad (2)$$

where;
f(x) is denotes the pixel value as an area unit.
w is the vertical values.
x is the horizontal values.
b is feature space.

2.2.3. Cloud fraction

A small cloud fraction indicates that there is more scattering in the atmosphere than computed based on the MODIS value. In the TROPOMI NO_2 emission, such small "cloud fractions" are used to implicitly compensate for aspects like too-small MODIS values (e.g. often the case over cities which have a higher reflectivity than the surroundings) or the presence of scattering aerosols, haze, or residual clouds. Ideally, the cloud pressure will indicate the altitude at which the scattering takes place (Mebust *et al*., 2016).

3. Results & Discussion

3.1. Spatial and Temporal distributions of NO_2 emission

MODIS and TROPOMI data to NO_2 emissions are provided in Figure (2). A minimum emission was 0.01 mg of NO_2 per month in order to discriminate and visualize the main emitters. NO_2 emissions are overlain as color-coded polygons, defined by the pixel corner coordinates provided in the Level2 product. However, elevated levels of NO_2 in the MODIS observations can be spatially resolved by TROPOMI and are averaged out within the TROPOMI pixel. The spatial resolution of the MODIS data allows revealing the scale NO_2 horizontal variability. The maps reveal that the NO_2 field is highly variable in both space and time. The NO_2 data by MODIS range were between 0.032 and 3.7×10^{-15} molec./cm^2 in study area. In KPP, NO_2 emissions are mainly related to industrial activities. Fine-scale plume from the KPP can be observed, the observed plume, narrow and confined close to the source; it is transported downwind for several tens of kilometers, as can also be observed in the TROPOMI data. The monthly average concentrations of NO_2 over the study area are shown in Figure (2).

ISSN (Print): 2413-5267
ISSN (Online): 2706-9966

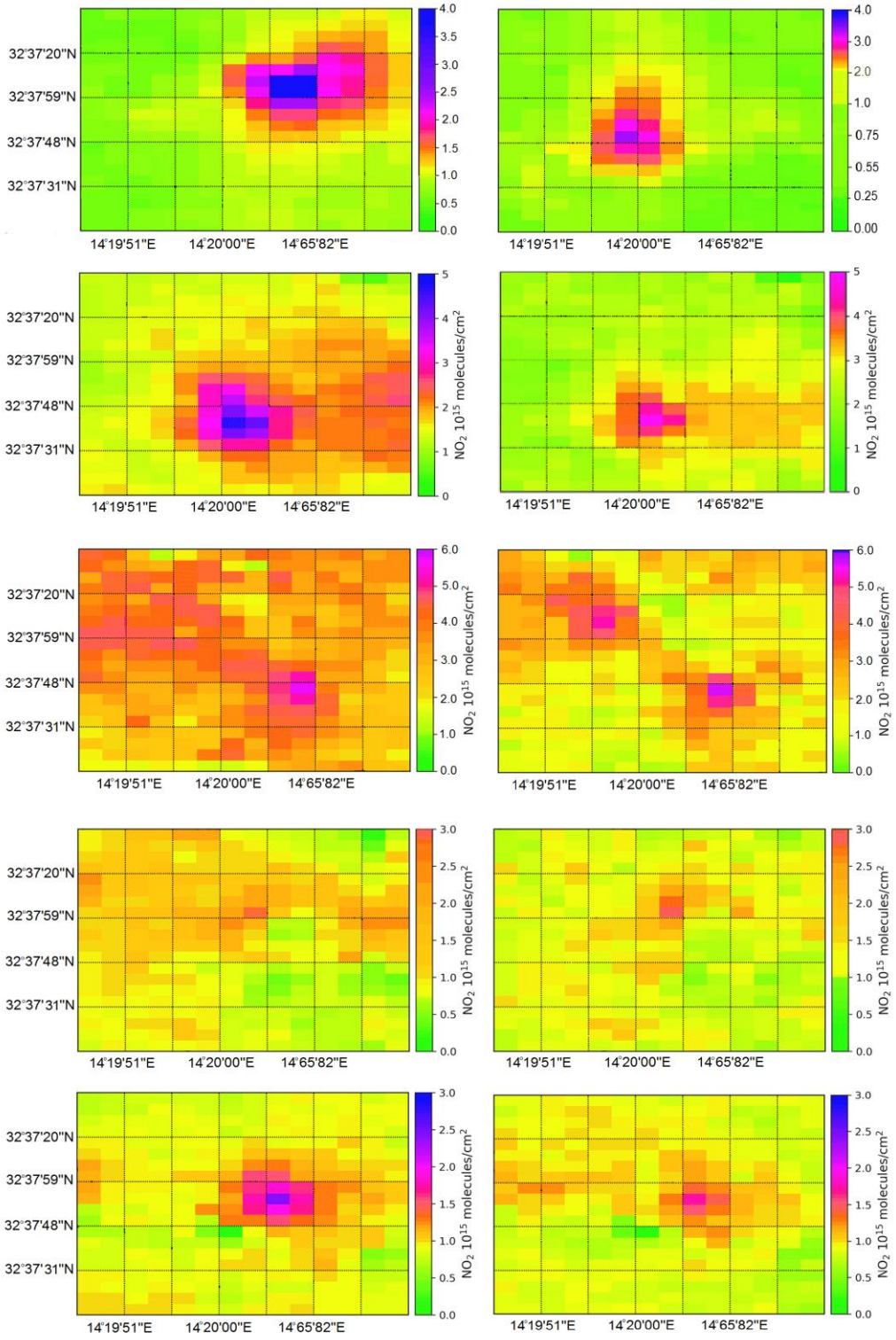

Figure 2. Showing left column represents TROPOMI observations, while right column indicate to MODIS images to NO_2 emissions monthly over study area on 2020. Note that different color bands, blue and red colors were representing high NO_2 concentrations. While NO_2 emission plume indicate to the surface wind direction.

ISSN (Print): 2413-5267
ISSN (Online): 2706-9966

The average monthly concentrations of NO_2 showed periodic changes throughout the year. In the months of July and August (that is, summer); NO_2 reached a minimum value of 2.15×10^{15} molec/cm^2, the values were in December and January (i.e., winter); NO_2 has a maximum value of 5.18 molecules/cm^2, in February the tropospheric column NO_2 concentration was fairly stable and showed some low fluctuations in the last months of the year 2020. TROPOMI observes a slightly lower NO_2 concentrations in June were $0.001 \pm 2.85\times10^{-15}$ molec./cm^2 and in January were $0.07\pm 4.32\times10^{-15}$ molec./cm^{-2}. The TROPOMI Level 2 tropospheric NO_2 product has been assessed based on independent high-resolution data, acquired over the target area. The accuracy of the tropospheric NO_2 emission recorded around 0.5×10^{15} molec./cm^{-2}. The effect of clouds was not considered in this study, as data acquisition took place in mostly clear-sky conditions.

The study area is characterized by many differences in land use, urbanization, agriculture, and industrialization. This means a difference in the brightness of the satellite image according to the size of the captured pixel, and thus these regions receive strong spatial contrast from the satellite data recordings of NO_2 emissions, especially beaches and steep spatial gradients. Where satellites capture their data using several wavelengths that vary in frequency depending on the type of target if is agricultural, industrial or residential. Thus, the measurement of pollution rate varies with the nature of that target. Although it's often has the same value when emitted into the atmosphere.

In this study, there was more pixel disturbance in the TROPOMI data due to the difference in the transverse path of the moon to capture the daily data, as a result of the intensity of the spectral reflection back on the satellite in the afternoon periods. This is illustrated in Figure (2) in violet from the source of nitrogen dioxide emissions. MODIS data show much more spatial detail when compared to TROPOMI data, as MODIS measures NO_2 peak values that are 3×10^{15} particles/cm^2 higher than TROPOMI monitors.

Nitrogen dioxide concentrations were categorized in different seasons from highest to lowest as follows: In winter, downward airflow prevails over cold weather. Thus, pollutants are not easily dispersed, which is one of the important factors in reducing air pollutants during winter (Guo *et al*., 2016). Moreover, the steam station area is located on a site that receives a great deal of rainfall in winter, and light rains occur in autumn. The annual distribution of precipitation is uneven, that is, from June to October, 90~95% rain drops, which plays a large role in reducing the amount of pollution. According to the research results, precipitation has little ability to remove air pollutants when the daily precipitation is less than 5 mm. However, when the daily precipitation exceeds 5 mm; the pollutant removal efficiency increases with increasing precipitation. The higher daily precipitation, the higher filtering rate and the better air quality. In addition, the maximum removal rate of air pollutants can reach 48.55% (Xiao *et al*., 2011). Precipitation affects the concentration of pollutants in the spring, summer, and fall, although air pollution is also influenced by industrial and human factors (Okasha *et al*., 2013; Okasha, 2014; and Cai, 2017).

ISSN (Print): 2413-5267
ISSN (Online): 2706-9966

3.2. Linear regression analyses

Regression line statistics are color coded blue for the comparison data. Note that vertical error bars indicate the overall errors in NO_2 (TROPOMI), while the horizontal whiskers represent the errors in NO_2 (MODIS). Data points are color coded based on the number of pixels, this is mean, TROPOMI pixels are more than 57 % pixels in all data. While in MODIS pixels were reference to 43% pixels, and all pixels are analyzed. Overall, positive relationship can be observed for both data (R^2= 0.87). For the NO_2 computation, the remaining disagreement between the both data sets can be potentially attributed to the following:

- There is disagreement due to different sensitivities to the NO_2 layer due to instrumental and algorithmic differences.
- There is disagreement due to differences in observation geometry and height.

In the event that there are temporal or spatial changes in the NO_2 field in the upper troposphere between the reference area and observed area, this should be implicitly measured. As the amount of NO_2 in the upper troposphere appears to be small compared to the total column over polluted sites, and as the MODIS retrievals still have some sensitivity to any impact on the comparisons to be minimal. There is disagreement due to temporal differences in the observation of a dynamic NO_2 field. MODIS data were acquired over the target areas, this is mean of the potential impact of temporal NO_2 variability due to the time offset between the MODIS and TROPOMI data. Relatively low and high biases occur at both small and large time offsets, which are pointing at a low impact of the temporal NO_2 variability under the current conditions. Due to the changes in the wind pattern, both data pixel footprints have different sizes. For example, on 13 February, 15 March, 09 April, 27 May, 26 September, 03 October, 02, 05, 09 and 22 November, additional to all December 2020, there was pollution not seen by MODIS satellite over the study area because of different pixels' size recorded to both data. This is meant different values from NO_2 concentration depend on pixel size. Scatter plots and linear regression analyses of TROPOMI and MODIS NO_2 data showed in Figure (3).

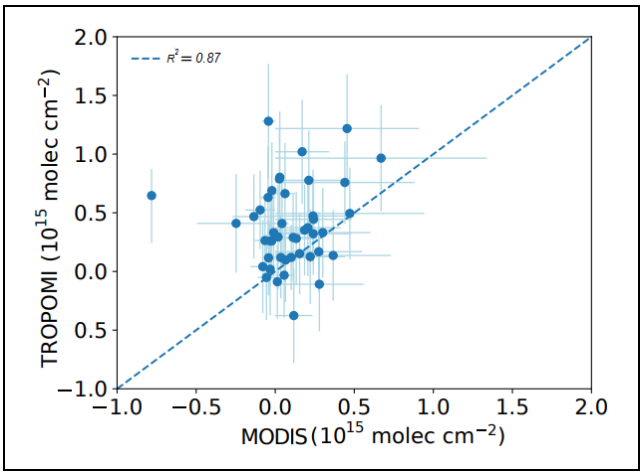

Figure 3. Scatter plots and linear regression analyses of average TROPOMI and MODIS data.

ISSN (Print): 2413-5267
ISSN (Online): 2706-9966

3.3. Support vector regression (SVR)

The spatial resolution (Figure 4) had a great role in detecting the pixel sizes associated with the emissions of nitrogen dioxide. Each of the pixels characterizes a certain concentration of nitrogen dioxide molecules. When recording MODIS observations, it was found that the pixels ranged from 00136 to 2853 millimeters, while the pixel of the TROPOMI monitor recorded 008 to 3062 millimeters. The accuracy of the degree of whiteness resulting from the intensity of spectral reflection or clouds recorded the pixel from -1003 to 005. Accuracy evaluation of these resulting pixels shows the extent of compatibility between both data in the pixel accuracy of the images of those different satellites in the size of the pixels differing in their correlation, the degree of brightness and time of shooting the image.

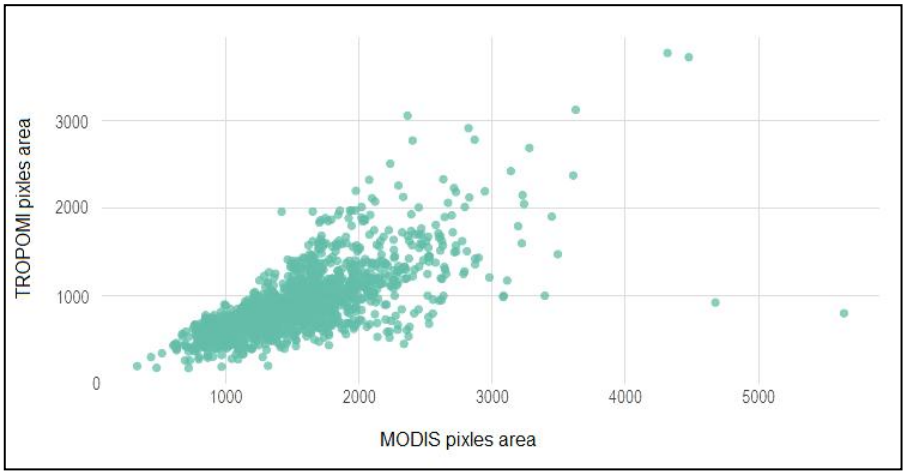

Figure 4. SVR to both data of pixel areas

3.4. Impact of pixel size

Emission measurement depends on the pixel size of satellite images, as we said earlier. This is done based on high-resolution MODIS observations and under active measurement of emitted NO_2 according to a medium technology within 1 km×1 km grid cells. The NO_2 rates are shown as in Figure (3) for the data set obtained from the study area. Scattered rates that are high in pixel pitch can be distinguished due to turbulence in the direction of the wind, when in reality it is easy to determine the direction of that wind. Note that the highest concentration of NO_2 levels is due to the strong effect of these pixels. In Figure (4), the pixel grid of the MODIS sensor, which was then monitored over the study area, indicates that nitrogen dioxide emissions were high when the sky was free of clouds, the brightness of the pixels is very high. This explains the intensity of the temporal relationship between the satellites measurements at the same time of each month of the study year. The lines between the dots indicate twice the brightness and therefore twice the recorded data. The wavelengths of NO_2 emissions allow us to further detect the concentration level of pollution by evaluating the highest values of emissions generated by the pixel resolution of satellite images, as shown in Figure (2), where the red band of pixels indicate the highest values of NO_2 emissions, while the blue band of

ISSN (Print): 2413-5267
ISSN (Online): 2706-9966

pixels indicate the highest values of NO_2 emissions. to low rates from nitrogen dioxide emissions. When increasing the pixel size, the NO_2 observations are low, while in case the pixel size decreasing NO_2 values are high. in this study showed that resolution of 1 km×1 km is a near-optimal resolution.

4. Conclusion

In order to prove that MODIS and TROPOMI data quality; this is one of the studies assessing NO_2 emissions over Khuoms city that resulting from gas power plant, impact pollution recorded in urban areas, based on the comparison between two satellites have high spatial accuracy. The NO_2 emissions that observed from MODIS, acquired on four seasons with clear-sky (2020), have been compared with TROPOMI observations. TROPOMI pixel has been covered by 230 to 1380 MODIS pixels. In this study the TROPOMI data were more accuracy from MODIS data, because of the difference in pixel size, and temporal resolution because of the amount of heterogeneity in the NO_2 field. Averaged over the four campaign seasons over study area, the average of the both data were estimated to be $3.6 \pm 0.4 \times 10^{15}$ molec./cm^2. The regression analysis was positive relationship ($R^2 = 0.87$). For quality studies at the city scale still require observations at higher spatial resolution by field studies or aircraft scanning, in order to assessment the typical heterogeneous NO_2 field. Results from the comparison with both data, have shown that the products meet the mission requirements in terms of accuracy. However, additional validation studies are required. Statistical models have a wide application and require less time to build models, but they require a large amount of historical data and have a high dependence on the long data time series approach. Statistic proved the satellite data and that forecast performance is better when considering the meteorological variables and the geographic factors. As the atmospheric environment is a complex system, there are many factors affecting the quality of the atmospheric environment, and the relationship between them is complicated. Therefore, air pollution forecasting based on the area and different pollutants should choose different forecasting methods. Moreover, there is no one best approach to make the most accurate forecast.

Acknowledgement

All my thanks and gratitude to the data sources for this research, including the Level-2 and Atmosphere Archive & Distribution System (LAADS) Distributed Active Archive Center (DAAC) for MODIS data, and the Copernicus ground system for the TROPOMI Level 2 data products and thanks to all references that helped me in this research plan.

ISSN (Print): 2413-5267
ISSN (Online): 2706-9966

References

Boersma K.F., Jacob D.J., and Bucsela E.J.(2018). Validation of OMI tropospheric NO_2 observations during INTEX-B and application to constrain NOx emissions over the eastern United States and Mexico. *Atmos. Environ. J.*, 42(19): 4480–4497.

Broccardo S., Heue K.P., Walter D., Meyer C., Kokhanovsky A., van der A.R., Piketh S., Langerman K., and Platt U. (2018). Intra-pixel variability in satellite tropospheric NO_2 column densities derived from simultaneous space-borne and airborne observations over the South African Highveld. *Atmos. Meas. Tech. J.*, 11: 2797-2819.

Cai W. (2017). Weather conditions conducive to Beijing severe haze more frequent under climate change. *Nat. Clim. Change, J.,* **7**: 257–262.

Compernolle S., Argyrouli A., Lutz R., and Sneep M. (2020). Validation of the Sentinel-5 Precursor TROPOMI cloud data with Cloudnet, MODIS. Available online at: [http://doi.org/10.5194/amt-122]

Constantin D.E. and Merlaud A. (2016). The AROMAT team: Airborne Romanian Measurements of Aerosols and Trace gases (AROMAT-II), *Final report, ESTEC, Noordwijk, The Netherlands*.

Dimitropoulou E., Hendrick F., Pinardi, and Van Roozendael M. (2020). Validation of TROPOMI tropospheric NO_2 columns using dual-scan MAX-DOAS measurements in Uccle, Brussels. *Atmos. Meas. Tech*., 1-50.

Friedl M.A., McIver D.K., Hodges J.C.F., Zhang X.Y., Muchoney D., and Schaaf C. (2017). Global land cover mapping from MODIS: algorithm and early results. *Remote Sens Env*., 83: 287–302.

Griffin D., Zhao X., McLinden, and Wolde M. (2019). High-Resolution Mapping of Nitrogen Dioxide with TROPOMI: First Results and Validation over the Canadian Oil Sands. *Geophys. Res. Lett*., 46(10):49–60.

Guo X.M. (2016). *Observation and Simulation of the Climate Characteristics of Air Quality and the Effects of Large Topography in Sichuan Basin*. Master's thesis, Nanjing University of Information Engineering, Nanjing, China.

Heue K.P., Wagner T., Broccardo S.P., Walter D., Piketh S.J., Ross K.E., Beirle S., and Platt U. (2018). Direct observation of two dimensional trace gas distributions with an airborne Imaging DOAS instrument. *Atmos. Chem. Phys. J.*, 8(67): 7–19.

Hong Z. and Hu F. (2015). Advances in theories and methods of air pollution prediction. *Clim. Environ. Res. J.*, 225–230

Huijnen V., Eskes H.J., and Poupkou A. (2016). Comparison of OMI NO_2 tropospheric columns 30 with an ensemble of global and European regional air quality models. *Atmos. Chem. Phys. J.*, 10: 10-32.

Ialongo I., Virta H., Eskes H., Hovila J., and Douros J. (2019). Comparison of TROPOMI/Sentinel 5 Precursor NO_2 observations with ground-based measurements in Helsinki. *Atmos. Meas. Tech. J.*, 3: 29-37.

ISSN (Print): 2413-5267
ISSN (Online): 2706-9966

Ibrahim H.G., Okasha, A.Y. Elatrash M.S. and Elmishregi M.A. (2012a). Emissions of SO_2, NOx and PMs from Cement Plant in Vicinity of Khoms City in North Western Libya, *Journal of Environmental Science and Engineering A1*, 620-628.

Ibrahim H.G., Okasha A.Y., Elatrash M.S., and Al-Meshraghi M.A. (2012b). Investigation of SO_2 and NOx Emissions from Khoms Power Stations in Libya. *International Conference on Environmental, Biomedical and Biotechnology*, 41: 191-195.

Ibrahim H.G., Elatrash M.S., and Okasha A.Y. (2011). Steam Power Plant Design Upgrading (Case Study: Khoms Steam Power Plant). *J. of Energy and Environment Research*, 1(1): 202-211.

Justice C.O., Townshend J.R.G., Vermote E.F., Masuoka E., Wolfe R.E., Saleous N., Roy D.P., and Morisette J.T. (2015). An overview of MODIS Land data processing and product status. *Remote Sens. Env. J.*, 83: 3–15.

Kim H.C., Lee P., Judd L., Pan L., and Lefer B. (2016). OMI NO_2 column densities over North American urban cities: the effect 20 of satellite footprint resolution. *Geosci. Model Dev. J.*, 9: 1111-1123.

Kleipool Q., Ludewig A., Babić L., and Veefkind P. (2018). Pre-launch calibration results of the TROPOMI payload on-board the Sentinel-5 Precursor satellite, *Atmos. Meas. Tech Journal*., 11: 439-479.

Lamsal L.N., Janz S.J., Krotkov N.A., and Herman J.R. (2017). High-resolution NO_2 observations from the Airborne Compact Atmospheric Mapper: Retrieval and validation: High-Resolution NO_2 Observations. *Journal of Geophysical Research: Atmospheres*, 122(3):1953– 1970.

Lawrence J.P., Anand J.S., Vande Hey J.D., White J., Leigh R.R., Monks P.S., and Leigh R.J. (2015). High-resolution measurements from the airborne Atmospheric Nitrogen Dioxide Imager (ANDI). *Atmos. Meas. Tech. J.*, 8: 4735–4754.

Mebust A.K., Russell A.R., Hudman R.C., Valin L.C., and Cohen R.C. (2016). Characterization of wildfire NO emissions using MODIS fire radiative power and OMI tropospheric NO_2 columns. *Atmos. Chem. Phys. J.*, 11: 5839–5851.

Morisette J.T., Privette J.L., and Justice C.O. (2012). A framework for the validation of MODIS Land products. *Remote Sens. Env. J.*, 83: 77–96.

Okasha A.Y. (2014). Main Industry Stack Emissions Dispersion Over Khoms City in North-Western Libya. *International Journal of Innovative Science, Engineering & Technology*, 1(10): 635-641.

Okasha A.Y., Hadia E.A., and Elatrash M.S. (2013). Ecological effect of Mergheb cement emissions on the vegetation in the Northwest Libya Here. *Inter. J. Sci.*, 2(9): 34-40.

Ortega I., Koenig T., Sinreich R., Thomson D., and Volkamer R. (2015). The CU 2-D-MAX-DOAS instrument Part1: Retrieval of 3-D distributions of NO and azimuth-dependent OVOC ratios. *Atmos. Meas. Tech. J.*, 8: 2371–2395.

Pinardi G., Van Roozendael M., Hendrick F., and Wittrock F. (2020). Validation of tropospheric NO_2 column measurements of GOME-2A and OMI using MAX-DOAS and direct sun network observations. *Atmos. Meas. Tech. J.*, 8: 61–85.

ISSN (Print): 2413-5267
ISSN (Online): 2706-9966

Platt U. and Stutz J. (2014). Differential absorption spectroscopy. In Differential Optical Absorption Spectroscopy. *Platt, Stutz, Journal*., Eds.; Springer: Cham, Switzerland,135–174.

Shi L., Xing L., Lu G., and Zou J. (2008). Evaluation of rational sulphur dioxide abatement in China. *Int. J. Environ. Pollut.,* 35: 42–57.

USEPA (2016). *Pollution* by *Nitrogen Dioxide (NO_2).* Available online at: [http://.epa.gov/no$_2$-pollution].

USEPA (2018). *Pollution* by *Nitrogen Dioxide (NO_2)* Available online at: [http://.epa.gov/no$_2$-pollution]

Van Geffen J.H.G.M., Eskes H., Pinardi G., Verhoelst T., Compernolle S., Sneep M., ter Linden M., Boersma K.F., and Veefkind J.P. (2020). S5P/TROPOMI NO_2 retrieval: impact of version V2.2 improvements and preliminary comparisons with OMI and ground-based data. *Atmos. Meas. Tech. J.*, 3: 49-57.

Van Noije T.P.C., Eskes H.J., Dentener F.J., Stevenson, D.S., Ellingsen K., Schultz M.G., and Roozendael, M. V. (2006). Multi-model ensemble simulations of tropospheric NO_2 compared with GOME retrievals for the year 2000. *Atmospheric chemistry and physics*, 6(10): 2943-2979.

Vasilkov A., Qin W., Krotkov N., Lamsal L., Spurr R., Haffner D., Joiner J., Yang E.-S., and Marchenko S. (2017). Accounting for the effects of surface BRDF on satellite cloud and trace-gas retrievals: a new approach based on geometry-dependent Lambertian equivalent reflectivity applied to OMI algorithms. *Atmos. Meas. Tech. J.*, 10: 333–349.

Williams J.E., van Zadelhoff G.J., and Scheele M.P. (2017). The effect of updating scavenging and conversion rates on cloud droplets and ice particles in the TM global chemistry transport model, *Technical Report TR-308, KNMI, De Bilt*.

Xiao Z. (2011). Study on the Characteristics of Atmospheric NO_2 in Sichuan Basin. *Chin. Environ. Sci. J.*, 31: 1782–1788.

Zhang Y., Bocquet M., Mallet V., Seigneur C., and Baklanov A. (2012). Real-time air quality forecasting, part I: History, techniques, and current status. *Atmos. Environ.*, 60: 632–655.

Zhao X., Griffin D., Fioletov V., McLinden C., Cede A., Tiefengraber M., Müller M., Bognar K., Strong K., Boersma F., Eskes H., Davies J., Ogyu A., and Lee S.C. (2020). Assessment of the quality of tropomi high-spatial-resolution No. 2 data products in the greater Toronto area. *Atmos. Meas. Tech. J.*, 13: 2131–2159.